Original Article

Apatinib inhibits pancreatic cancer growth, migration and invasion through the PI3K/AKT and ERK1/2/MAPK pathways

Yuan Hu[1], Jiayu Jing[2], Yu Shi[1], Pengchuang Zhang[3], Danfeng Dong[1], Yinying Wu[1], Xuyuan Dong[1], Enxiao Li[1#], Yangwei Fan[1#]

[1]Department of Medical Oncology, The First Affiliated Hospital of Xi'an Jiaotong University, Xi'an, China; [2]Department of Medical Ultrasonics, The Second Affiliated Hospital of Xi'an Jiaotong University, Xi'an, China; [3]Department of Gynecologic Oncology, Shaanxi Provincial Tumor Hospital, Xi'an, China

Contributions: (I) Conception and design: E Li, Y Fan; (II) Administrative support: Y Wu, X Dong; (III) Provision of study materials or patients: D Dong; (IV) Collection and assembly of data: J Jing, Y Shi; (V) Data analysis and interpretation: Y Hu, P Zhang; (VI) Manuscript writing: All authors; (VII) Final approval of manuscript: All authors.

[#]These authors contributed equally to this work.

Correspondence to: Dr. Yangwei Fan; Prof. Enxiao Li. Department of Medical Oncology, The First Affiliated Hospital of Xi'an Jiaotong University, 277 Yanta West Road, Xi'an 710061, China. Email: 1159950306@qq.com; doclienxiao@sina.com.

Background: Pancreatic cancer is generally characterized with high levels of malignancy and poor prognosis. In addition, there are currently no effective therapeutic agents against the disease. However, apatinib which is a small molecular agent targeting the vascular endothelial growth factor receptor 2 (VEGFR-2), has been shown to generate favorable outcomes in gastric cancer. Therefore, the present study explored the effects of apatinib on pancreatic cancer.

Methods: The activity of the ASPC-1 or PANC-1 cells was examined through colony formation assays, wound healing experiments as well as the Transwell and Western blot (WB) analyses. Additionally, a xenograft model was established by subcutaneously injecting the ASPC-1 cells into nude mice. Microvessel density (MVD) and Ki-67 expression were examined through immunohistochemistry (IHC) and WB analyses.

Results: The findings showed that treatment with either 10 or 20 μM of apatinib led to a decrease in the proliferation, migration and invasion of ASPC-1 and PANC-1 cells. Additionally, apatinib significantly hindered xenograft growth. Moreover, there was a decrease in Ki-67 expression and MVD, 21 days after treatment with apatinib. The results also showed that apatinib had no effect on the levels of the VEGFR-2, ERK1/2 and AKT proteins although there was a significant decrease in the expression of phosphate VEGFR2 (p-VEGFR2), phosphate AKT (p-AKT) and phosphate ERK1/2 (p-ERK1/2).

Conclusions: Apatinib inhibits the proliferation and migration of pancreatic cancer cells, blocking growth and angiogenesis in transplanted tumors. In addition, the underlying mechanism may involve phosphorylation of the PI3K/AKT and ERK1/2/MAPKs signaling pathways.

Keywords: Pancreatic cancer; apatinib; vascular endothelial growth factor receptor 2 (VEGFR-2); ERK1/2; AKT

Submitted Jan 31, 2021. Accepted for publication May 25, 2021.
doi: 10.21037/tcr-21-207
View this article at: https://dx.doi.org/10.21037/tcr-21-207

Introduction

Pancreatic cancer is among the most stubborn malignant tumors, with many patients only showing general symptoms such as abdominal pain or weight loss (1,2). This non-specificity delays the diagnosis of the disease, resulting in nearly 80% of patients being diagnosed at an advanced stage (3) and missing the opportunity for early surgical resection of the tumors. Nonetheless, the 5-year survival rate

of patients receiving operations is only 25% (4). Additionally, treatments such as radiotherapy and chemotherapy have limited benefit in pancreatic cancer. Notably, the recently developed treatment using gemcitabine prolongs the overall survival time, but only with 1 to 2 months (5). Moreover, in-depth studies of the tumor microenvironment and challenges in surgical treatment, chemotherapy and radiotherapy, revealed that molecular targeting strategy and immunotherapy may be the only alternatives for treating pancreatic cancer (6).

Angiogenesis is a crucial step in the growth, invasion and metastasis of solid tumors. The process provides a conducive environment for oxygen and nutrient transportation, waste metabolization and long-distance transfer of cancer cells (7). Additionally, the vascular endothelial growth factor (VEGF) acts on the vascular endothelial growth factor receptors 1 and 2 (VEGFR-1 and VEGFR-2) to promote the proliferation, migration and neovascularization of endothelial cells, ultimately mediating angiogenesis in various tumors (8-10). In ovarian cancer, VEGF plays a key role in both tumor aggression towards surrounding tissues and generation of malignant ascites following peritoneal metastasis. Angiogenesis also facilitates the progression of pancreatic cancer and inhibition of the process could be a promising approach for tumor stabilization (11).

In addition, apatinib (YN968D1) is an oral tyrosine kinase inhibitor that was developed in China. Apatinib selectively blocks the intracellular binding sites of adenosine triphosphate in VEGFR-2, subsequently preventing the receptor from being phosphorylated (12,13). Notably, this agent was approved by the China Food and Drug Administration (CFDA) in 2014 for use in the treatment of patients with advanced gastric cancer or gastroesophageal junction adenocarcinoma. Moreover, apatinib significantly reduces the formation of vascular structures and inhibits tumor growth in breast cancer, non-small cell lung cancer and colorectal cancer (14-17). Nevertheless, the effect of apatinib on pancreatic cancer and the underlying molecular mechanisms remain unclear. Therefore, the current study aimed to explore the effects of apatinib on pancreatic cancer cells and xenograft tumors grown in nude mice. The results showed that apatinib inhibited the proliferation and migration of pancreatic cells, blocking growth and angiogenesis in transplanted tumors. The findings also revealed that this process may be related to the decreased phosphorylation of the PI3K/AKT and ERK1/2/MAPK signaling molecules. We present the following article in accordance with the ARRIVE reporting checklist (available at https://dx.doi.org/10.21037/tcr-21-207).

Methods

Cell culture and reagents

The study was conducted in accordance with the Declaration of Helsinki (as revised in 2013). Two human pancreatic cancer cell lines, ASPC-1 and PANC-1 (Genechem BioTECH, Shanghai, China) were cultured in the RPMI-1640 (HyClone) and DMEM (HyClone) media, respectively, at 37 ℃ in a humidified atmosphere with 5% CO_2. The culture media consisted of fetal bovine serum (FBS, 10%, HyClone, Logan, UT, USA), streptomycin (100 μg/mL, Life Technologies, Grand Island, NY, USA) and penicillin (100 U/mL). In addition, apatinib was obtained from the Jiangsu Hengrui Medicine Co., Ltd. (Jiangsu, China).

The sulforhodamine B (SRB) assay

Cells were placed in individual wells, adjusted to a density of 5×10^3 cells/well then left overnight for adherence. Thereafter, the cells were incubated in a blank vehicle [dimethyl sulfoxide (DMSO); Sigma-Aldrich, St. Louis, MO, USA] or seven concentration gradients of apatinib (μmol/L: 1.56256, 3.125, 6.25, 12.5, 25, 50 and 100). Afterwards, 50 μL of pre-cooled 50% (w/v) Trichloroacetic Acid (TCA) solution was added for fixation at 4 ℃ for 1 h. In addition, 100 μL of 0.4% (w/v in acetic acid) SRB (Sigma-Aldrich) solution was used to stain the cells at room temperature for 10 min in the dark. The optical density (OD) of each well was detected on a microplate reader (Bio-Rad, Hercules, CA, USA) at 540 nm and the cell inhibition rate was calculated according to Eq. [1].

$$Cell\ Inhibition = 1 - \frac{OD_{Test}}{OD_{Negative\ Control}} \times 100 \quad [1]$$

Moreover, the GraphPad Prism software (version 8.0, GraphPad, Inc., San Diego, CA, USA) was used to draw a dose-response curve for calculating the half-maximal inhibitory concentration (IC_{50}) value of apatinib in different cancer cells.

The plate clone formation assay

Cells were seeded in 6-well plates containing 3 mL of complete medium at a density of 300 cells/well. In addition, apatinib (10 or 20 μM) or DMSO was added, after which the cells were incubated for 72 h. Thereafter, the cells

were collected and cultured in a drug-free medium for 2–3 weeks. The cells were then fixed with 2 mL of 4% paraformaldehyde for 10 min, after being washed thrice in PBS. Afterwards, 1 mL of 0.1% (w/v in PBS) crystal violet was added to stain the cells for 30 min. Pictures were then taken and the visible colonies (>50 cells) were manually counted. Notably, the relative clone formation ability was defined as the mean experimental number of clones divided by the mean number of clones in the control.

The Transwell assay

In order to evaluate cell invasion and migration, Transwell plates (8-μm pore size, Corning) with a polycarbonate filter were coated with or without 50 μL of the Matrigel matrix (BD Biosciences; 1: 6 dilution). Transwell chambers were then placed in a 24-well plate, after which 600 μL of complete medium and 200 μL of cell suspension (5×10^4) were drawn into the lower and upper chambers, respectively. After incubation at 37 ℃ for 72 h, the cells that crossed the basement membrane (in the migration assay) or Matrigel (in the invasion assay) and adhered to the lower chamber were fixed with 4% paraformaldehyde (w/v) for 30 min, followed by staining with 500 μL of 0.1% crystal violet for another 30 min. Photographs were then taken under a microscope (Nikon-Eclipse). Additionally, cells in five randomly selected fields were counted at 200× magnification to represent the number of transmembrane cells.

The wound healing assay

After pretreating the cells that adhered to the walls, scratches were made using a sterilized 10 μL pipette tip. In addition, the wound area was measured before and after 72 h of culture in serum-free media. Notably, three sites of the wound were selected on each plate, after which they were measured and averaged. Photographs were then taken under a microscope (Nikon-Eclipse) at 100× magnification. Moreover, wound closure was evaluated based on Eq. [2] where L_t and L_0 indicated the wound area at 24 h and 0 h, respectively.

$$Wound\ Closure = 1 - \frac{L_t}{L_o} \quad [2]$$

The xenograft model

The model was created using 20 male thymless BALB/c nude mice aged 4–6 weeks and weighing 18–20 g (Shanghai Laboratory Animal Center of the Chinese Academy of Sciences). The mice were housed in the animal center of the Medical College of Xi'an Jiaotong University in a specific pathogen-free environment. Experiments were performed under a project license (No. XJTU1AF2015LSL-063) granted by the ethics committee of the First Affiliated Hospital of Xi'an Jiaotong University, in compliance with the national or institutional guidelines for the care and use of animals. Briefly, ASPC-1 cells (1×10^7 cells) were re-suspended in PBS, then mixed with Matrigel, which was injected into the right thigh of mice to establish subcutaneous xenograft models of pancreatic cancer. Additionally, the body weight and tumor volumes of each animal were recorded every two days during the entire period of tumor growth. Moreover, the mice were randomly allocated into four groups (five per group) when the average volume of the tumor reached 100–300 mm^3. The groups included; the apatinib high-dose group (200 mg/kg p.o. qd ×21), apatinib middle-dose group (100 mg/kg p.o. qd ×21), apatinib low-dose group (50 mg/kg p.o. qd ×21) and normal saline (NS) group (18). In addition, tumor volume was estimated every three days according to Eq. [3]; where a and b denoted the largest and smallest diameter of the tumor, respectively.

$$V\left(cm^3\right) = a \times \frac{b^2}{2} \quad [3]$$

Twenty-one days later, the mice were sacrificed and the tumor tissue was collected. Part of the tumor tissue was then fixed in 10% formalin for pathological tests while the remaining portion was frozen in liquid nitrogen.

The immunohistochemistry (IHC) assay

The study prepared 4 μm thick tissue sections which were then incubated overnight at 65 ℃. Thereafter, antigen recovery was performed using 10 mM of citrate buffer followed by IHC staining using a streptavidin-biotin peroxidase kit (SP-9001, Zhongshan Golden Bridge Biotechnology, Beijing, China) according to the manufacturer's instructions. In addition, anti-CD31 antibodies (1:500, 11265-1-AP, Proteintech, Wuhan, China) or PBS were added then the slides were placed in a humid incubation chamber, overnight at 4 ℃. The intensity of expression was quantified as the ratio of the integrated optical density (IOD) of the areas of interest (AOIs) to that of the background using the IPP 6.0 software (Media Cybernetics).

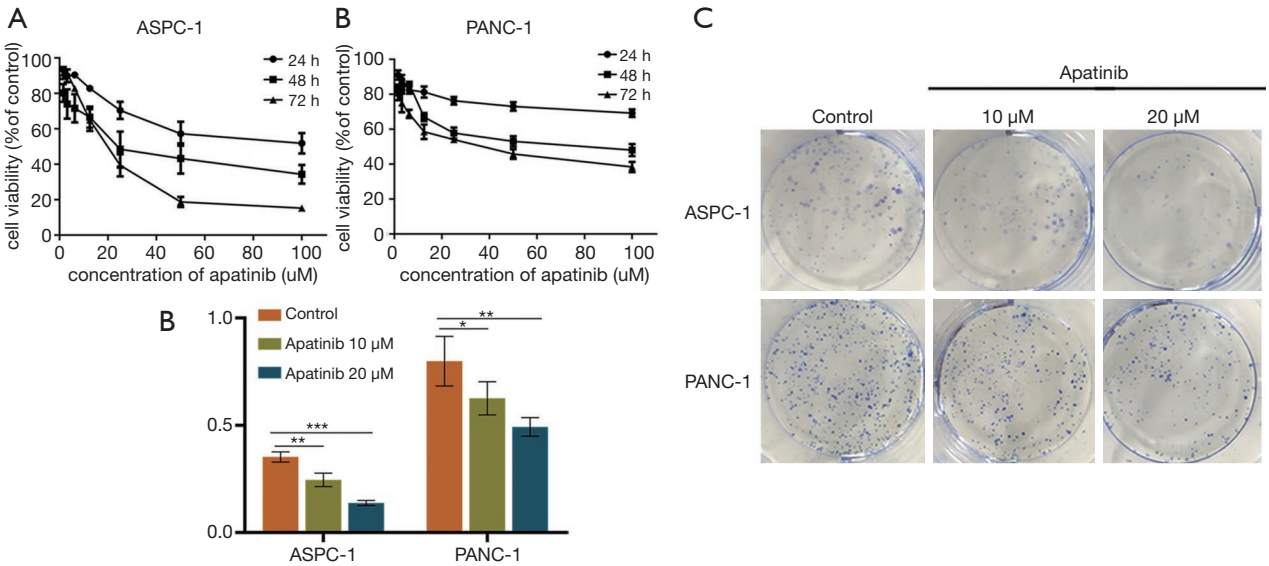

Figure 1 Apatinib inhibited cell viability and proliferation in a dose- and time-dependent manner. SRB assay showing growth curves of ASPC-1 cells (A) and PANC-1 cells (B) treated with different doses (0, 20, 40, 60, 80, 100 μM) of apatinib for different periods of time (24, 48, 72 h). Representative images (C) and summarized data (D) of a colony formation assay exhibiting the proliferation of ASPC-1 and PANC-1 cells. Data are presented as mean ± SD (n=5). *, P<0.05; **, P<0.01; ***, P<0.001 (n=3) *vs.* control group. SRB, sulforhodamine B.

Western blot (WB) analysis

The cells or frozen tumor tissues were homogenized on ice with a pre-chilled lysis buffer containing protease and phosphatase inhibitors (Roche, Indianapolis, IN, USA). Thereafter, centrifugation was performed at 4 ℃ for 30 min, after which the supernatant was collected. The concentration of proteins was then examined using a bicinchoninic acid protein assay kit (Thermo Fisher Scientific, Waltham, MA, USA; 23227). In addition, an equivalent amount of protein was added and separated in a sodium dodecyl sulphate-polyacrylamide gel. Thereafter, the protein was transferred onto a polyvinyl difluoride membrane (Millipore Corp., Boston, MA, USA) and blocked in 5% (w/v) skim milk for 2 h, at room temperature. This was followed by incubation with a primary antibody at 4 ℃, overnight then treatment with the HRP-conjugated secondary antibody (Cell Signaling Technology, Boston, MA, USA; #7044; diluted at 1:5,000) for 1 h at room temperature. Afterwards, the blots were visualized using an enhanced chemiluminescence kit (Millipore Corp, Boston, MA, USA). Moreover, GAPDH (1:5,000, HRP-60004, Proteintech, Wuhan, China) was chosen as the internal control. The following primary antibodies were used: VEGFR-2 (1:1,000, 9698S, CST), phosphate VEGFR2 (p-VEGFR2; 1:1,000, 2478S, CST); AKT (1:500, WL0003b, Wanleibio, Shenyang, China), phosphate AKT (p-AKT; 1:500, WLP001a, Wanleibio, Shenyang, China), ERK1/2 (1:1,000, 29162, SABbiotech) and phosphate ERK1/2 (p-ERK1/2; 1:1,000, 12548, SABbiotech).

Statistical analysis

Statistical analysis and plotting were performed using the SPSS software (Statistical Package for the Social Sciences version 18.0) and GraphPad Prism software (version 8.0), respectively. The data was expressed as mean ± SD. In addition, differences between groups were analyzed using one-way ANOVA and the least-significant difference (LSD) post hoc analysis. All statistical tests were two-sided with a 5% level of significance.

Results

Apatinib reduced the vitality and proliferation of pancreatic cancer cells

The IC_{50} of apatinib against the ASPC-1 and PANC-1 cells at 72 h was 16.94 and 37.24 μM, respectively (*Figure 1*). Based on these results, 10 and 20 μM of apatinib were used in the subsequent assays. Additionally, the control ASPC-1 cells had a colony formation rate of 35.22%±2.34%, which was

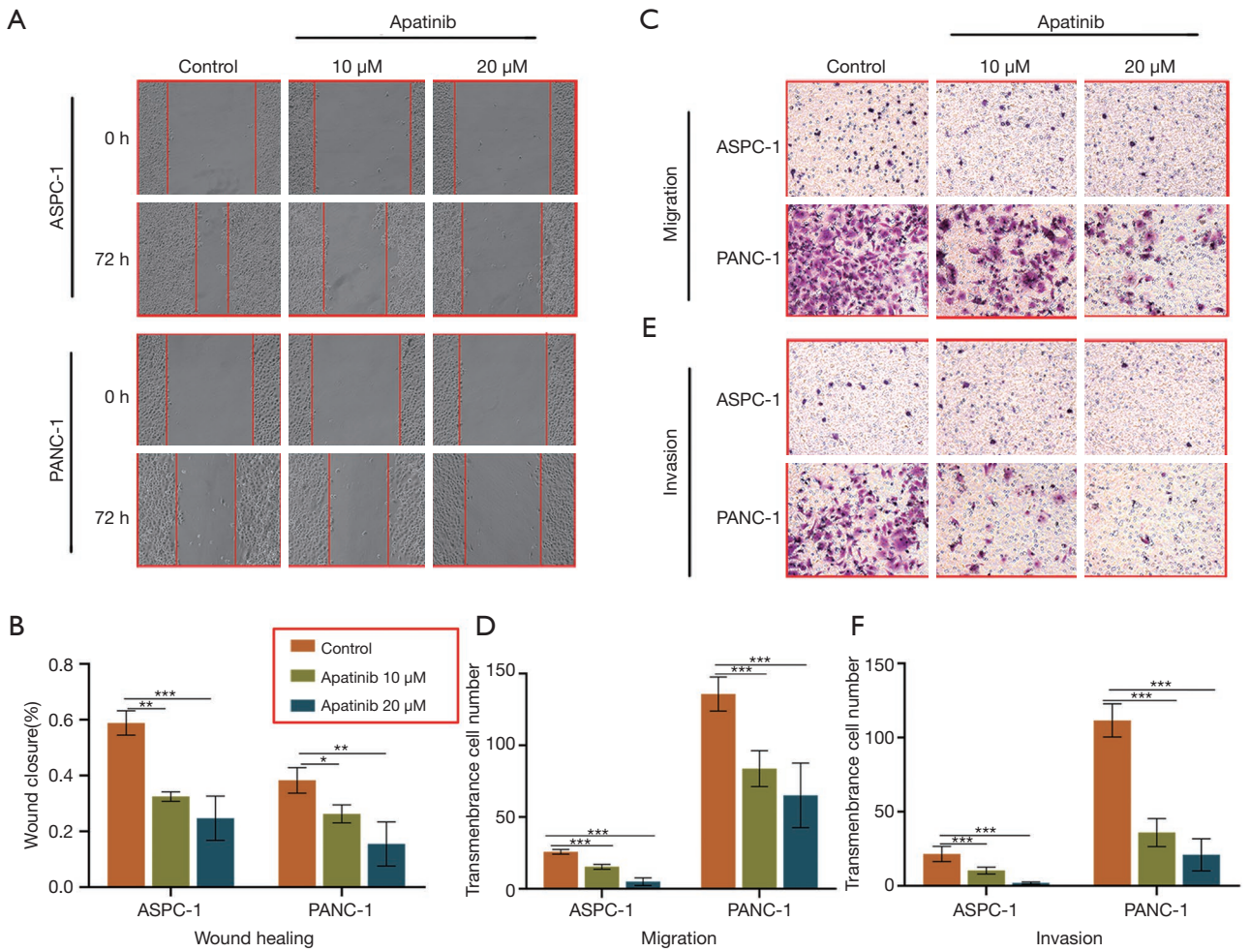

Figure 2 Apatinib prevented the migration and invasion in ASPC-1 and PANC-1 cells. Representative images (A,C,E) and summarized data (B,D,F) showing wound healing and Transwell assays on ASPC-1 or PANC-1 cells treated by vehicle (control), 10 or 20 μM apatinib. Three sites of the wound were selected on each plate, and photographs were taken under a microscope (Nikon-Eclipse) at 100× magnification. The Transwell assay was stained with 0.1% crystal violet. Data are presented as mean ± SD (n=3). *, P<0.05; **, P<0.01; ***, P<0.001 (n=3) *vs.* control group.

significantly higher than the 24.56%±3.15% observed in the cells treated with 10 μM of apatinib (P=0.001, *Figure 1C,D*) and the 13.78%±1.17% observed in the 20 μM of apatinib (P=0.000). Similarly, the control PANC-1 cells had a colony formation rate of 79.89%±11.61%, which was significantly higher than that in cells treated with 10 μM (62.56%±7.72%; P=0.045) and 20 μM of apatinib (49.22%±4.34%; P=0.004).

Apatinib suppressed the migration and invasion of pancreatic cancer cells

Migration and invasion of cancer cells are critical for tumor metastasis. Therefore, the study assessed the migration and invasion of cancer cells using the Transwell and wound-healing assays, respectively. The findings revealed that 72 h of incubation with 20 or 10 μM of apatinib significantly reduced wound closure in both the ASPC-1 (20 μM, 24.68%±7.93%, P=0.001 and 10 μM, 32.49%±1.70%, P=0.001 *vs.* 58.85%±4.35%) and PANC-1 cells (20 μM, 15.49%±7.90%, P=0.002 and 10 μM, 26.25%±3.24%, P=0.001 *vs.* 38.28%±4.57%), compared to the controls (*Figure 2A,B*).

Moreover, the Transwell assay without the matrigel was used to examine cell migration. The results showed that

treating both the ASPC-1 and PANC-1 cells with 20 μM (5.00±2.74, P=0.000; 65.20±22.49, P=0.000) or 10 μM of apatinib (15.40±1.67, P=0.000; 83.80±12.46, P=0.000) for 72 h significantly reduced cell migration (*Figure 2C*), relative to the controls (25.80±1.63; 135.8 ± 11.90; *Figure 2D*).

On the other hand, Transwell assays with the matrigel demonstrated the invasive ability of the cancer cells. Notably, 10 μM (10.40±2.30, P=0.000) or 20 μM (2.00±0.71, P=0.000) of apatinib significantly reduced the number of transmembrane ASPC-1 cells (*Figure 2E*), compared to the controls (21.60±5.13, *Figure 2F*). Similar results were obtained from the PANC-1 cells. Additionally, the control group had more transmembrane cells (111.60±11.20) than the category treated with either 10 μM (36.00±9.46; P=0.000) or 20 μM (21.00±10.84; P=0.000) of apatinib.

Apatinib inhibited cell-derived xenograft growth

In order to evaluate the anti-tumor effect of apatinib *in vivo*, subcutaneous xenografts of nude mice were established and observed. The findings showed that mice treated with any dose of apatinib had insignificant weight loss by the end of the investigation. In addition, the high-dose apatinib group had a lower tumor volume than that the NS category, 12 days after treatment (P=0.013) although the difference was not significant across the groups. However, there was a significant difference in tumor volume between the four groups (*Figure 3A,B*, P=0.028), fifteen days after treatment. Moreover, there was a significant difference in tumor volume between the middle-dose and NS groups, from day 18 to the end of the experiment (P=0.008). Overall, there was a significant difference in tumor volume between the high- and middle-dose groups as well as between the middle- and low-dose categories.

Apatinib inhibited the angiogenesis and proliferation of tumors

In this study, hematoxylin-eosin (HE) was stained to show representative tumor tissue (*Figure 3C*), CD31 was stained to visualize the vascular endothelial cells and Ki-67 was examined to indicate proliferation. The results showed that the high-dose (P=0.000), middle-dose (P=0.003) and low-dose (P=0.034) apatinib treatments all significantly reduced the expression of the CD31, compared to the NS group (*Figure 3D,E*). Moreover, the intensity of Ki-67 in the NS group was significantly higher than that in the high-dose (P=0.000), middle-dose (P=0.000) or low-dose (P=0.004) apatinib-treatment groups (*Figure 3D,F*).

Apatinib inhibited the ERK1/2/MAPKs and PI3K/AKT signaling pathways

It is known that apatinib inhibits VEGFR-2 and modulates both the ERK1/2/MAPKs and PI3K/AKT pathways. Based on these mechanisms, the present study examined the associated molecular signals, *in vitro* and *in vivo* (*Figure 4*). The results in *Figure 4A,D* show that apatinib significantly down-regulated the phosphorylation of VEGFR-2 in pancreatic cancer cells (ASPC-1, P=0.000; PANC-1, P=0.001) and tumor tissue (P=0.000). Furthermore, treatment with either 20 μM or 10 μM of apatinib reduced the expression of p-AKT in both the ASPC-1 (P=0.000; P=0.000) and PANC-1 cells (P=0.000; P=0.044) as shown in *Figure 4A,B,C*. The findings also showed that apatinib reduced the levels of p-AKT was in the tumor tissues of mice (all doses, P=0.000) compared to treatment with NS (*Figure 4D,E*). With regard to the ERK1/2/MAPKs pathway, the levels of p-ERK1/2 were lower in apatinib-treated ASPC-1 (P=0.003) and PANC-1 (P=0.001) cells than in the controls (*Figure 4A,B,C*). The cell-derived xenograft tissues treated with different doses of apatinib also showed reduced expression of p-ERK1/2, compared to those treated with NS (*Figure 4D,E*, P=0.004). Furthermore, both the *in vitro* and *in vivo* experiments showed that the total protein levels of VEGFR-2, ERK1/2 and AKT were unaffected by apatinib.

Discussion

In the present study, both the *in vitro* and *in vivo* experiments confirmed that apatinib suppresses the proliferation, migration and invasion of pancreatic cancer cells, mitigating the growth of xenografts and lowering microvessel density (MVD) as well as expression of Ki-67. Moreover, apatinib reduced the expression of p-VEGFR2, p-AKT and P-ERK1/2 but not the levels of the VEGFR-2, AKT and ERK1/2 proteins.

Few studies have been conducted to examine the effect of apatinib on pancreatic cancer. For instance, He *et al.* (19) showed that apatinib inhibited the proliferation and migration of CFPAC-1 and SW1990 pancreatic cancer cells *in vitro* and reduced the expression of p-AKT. Although the present study used the ASPC-1 and PANC-1 cell lines, the results similarly highlighted the inhibitory effect of apatinib on pancreatic cancer *in vitro*. In addition, the present

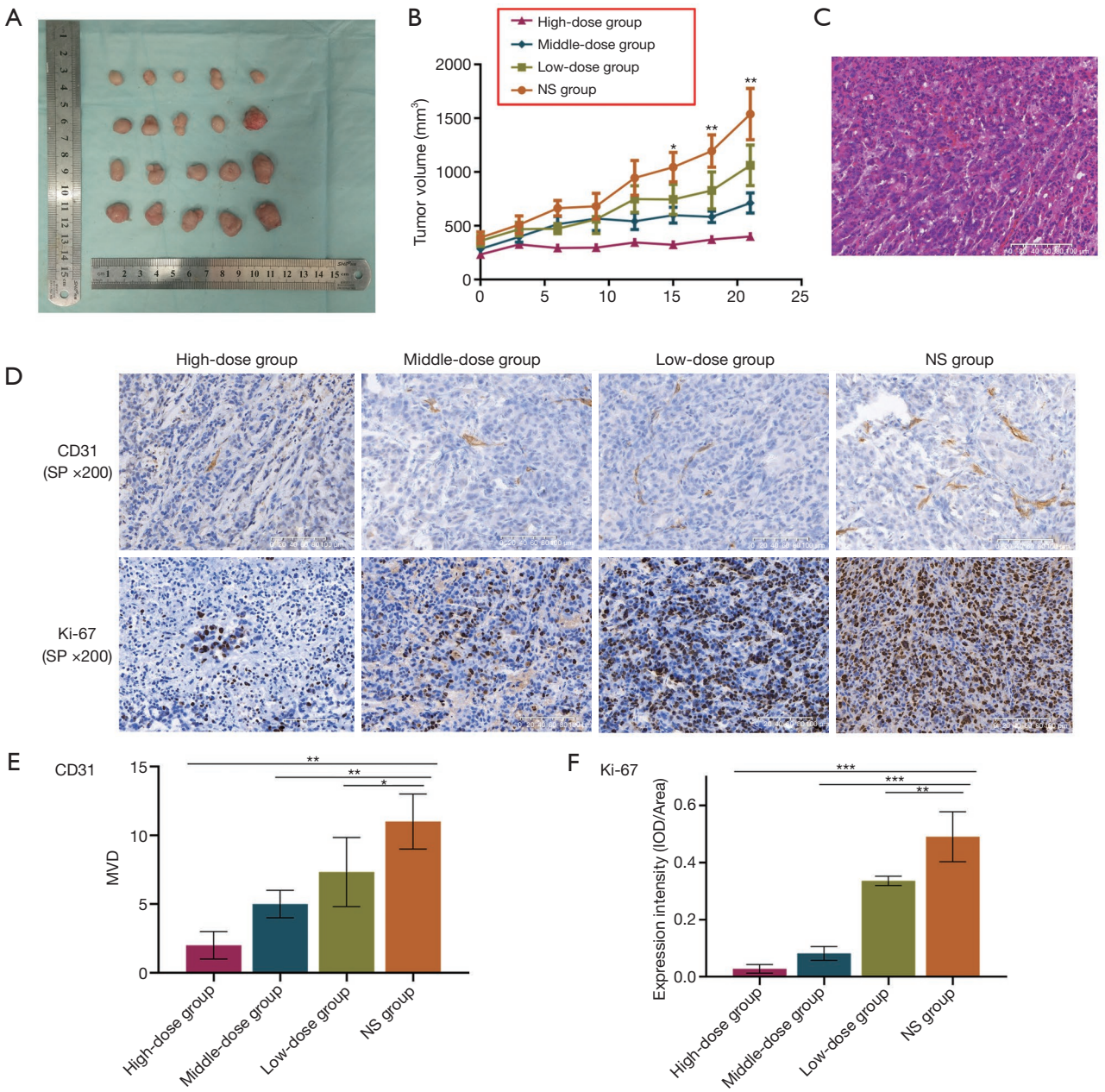

Figure 3 Apatinib suppressed tumor growth, angiogenesis and proliferation of pancreatic cancer xenografts in nude mice. Representative images and summarized data of tumor volumes (A,B), HE (C) and IHC staining for the detection of CD31 (D,E) or Ki-67 (D,F) in nude mice treated with NS, low-dose (50 mg/kg), middle-dose (100 mg/kg) or high-dose (200 mg/kg) apatinib. Magnification: ×200. Data are shown as mean ± SD (n=3). *, P<0.05; **, P<0.01; ***, P<0.001 *vs.* NS group. HE, hematoxylin-eosin; IHC, immunohistochemistry; NS, normal saline; MVD, microvessel density; IOD, integrated optical density.

study tested the effect of apatinib on the invasive ability of cancer cells. The findings revealed that in addition to the reported inhibitory effects on proliferation, migration and apoptosis, apatinib also inhibits the invasion of pancreatic cancer cells. This was similar to the results obtained from a previous study where pancreatic cancer cells were treated with a combination of apatinib and the traditional Chinese medicine, the astragalus polysaccharide (20). The results in

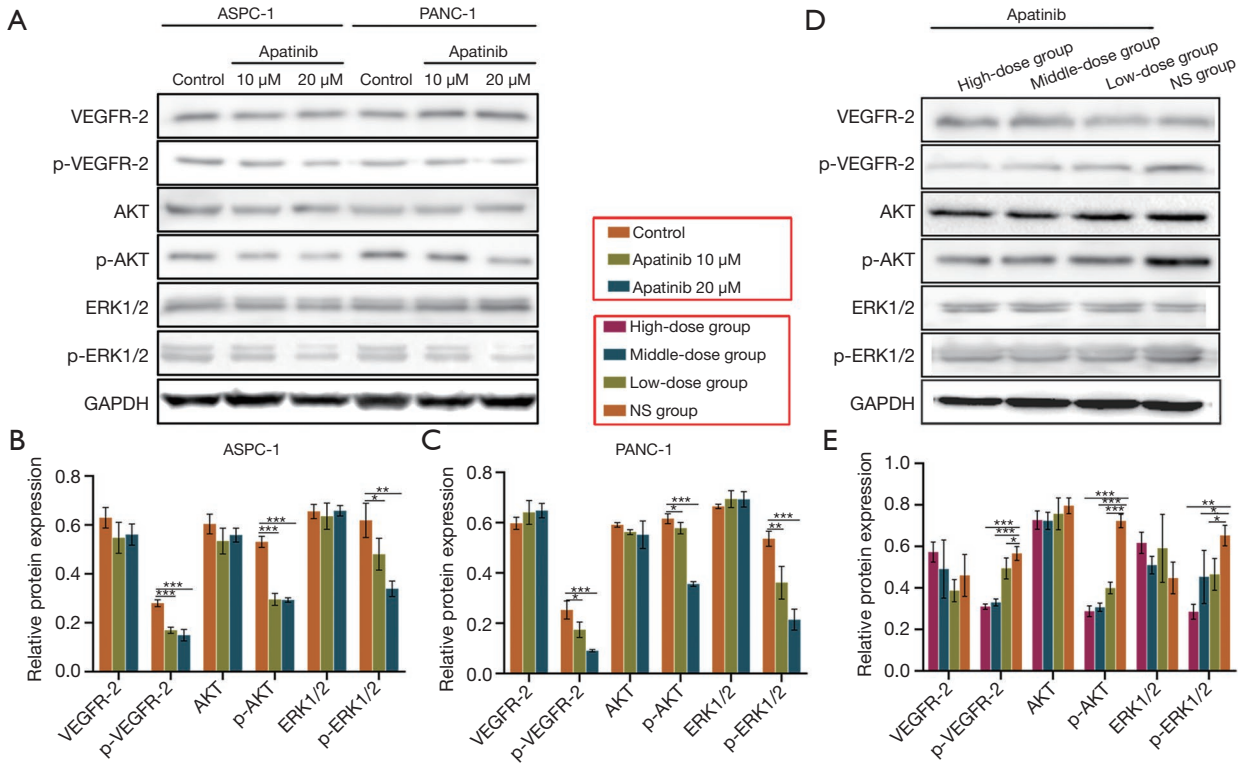

Figure 4 Apatinib restrained activation of the PI3K/Akt and ERK1/2/MAPK pathway in pancreatic cancer cells and xenografts. Representative images and summarized data showing WB analysis of VEGFR-2, p-VEGFR-2, AKT, p-AKT, ERK1/2 and p-ERK1/2 in ASPC-1 or PANC-1 cells (A,B,C) and in nude mice treated with NS, low-dose, middle-dose or high-dose apatinib (D,E). Data are shown as mean ± SD (n=3). *, P<0.05; **, P<0.01; ***, P<0.001 *vs.* control or NS group. WB, Western blot; VEGFR-2, vascular endothelial growth factor receptor 2; p-VEGFR-2, phosphate VEGFR-2; p-AKT, phosphate AKT; p-ERK1/2, phosphate ERK1/2; NS, normal saline.

the study showed that the proliferative ability and invasion of ASPC-1 and PANC-1 cell lines were substantially inhibited *in vitro*. However, this study did not compare the difference between differrent concentrations. In the present study, apatinib showed a similar inhibitory effect in a dose dependent manner. Moreover, previous *in vitro* studies confirmed the anti-angiogenetic potential of apatinib in esophageal cancer (21), cholangiocarcinoma (22), colon cancer (23), osteosarcoma (24) and other well-tolerated tumors. The anti-angiogenetic effect of apatinib on pancreatic cancer may be related to the high expression of VEGFR-2 in pancreatic cancer cells (25,26) or the existence of other targets of the drug. This indicates that apatinib is not only able to suppress tumor growth by decreasing angiogenesis but also by directly controlling many solid tumors.

Moreover, the present study for the first time showed that apatinib inhibited tumor growth and substantially reduced tumor volume in the xenografts derived from pancreatic cancer cells. This effect occurred in a dose- and time-dependent manner, with higher doses and longer durations of treatment causing more visible consequences. However, there was no significant difference between two adjacent groups, probably due to the relatively small differences (two times) in the concentrations of apatinib. Nevertheless, the efficacy of anti-angiogenic drugs does not always occur in a dose-dependent manner, because the excessive vascular suppression induced by over-dosing results in an increasingly hypoxic environment that accelerates tumor growth. Therefore, the dose-dependence presented in this study actually refers to a certain concentration range, rather than the idea that a higher concentration of apatinib leads to better control of pancreatic cancer. Given this nonlinear relationship, the optimal dose of apatinib needs to be determined through further experiments.

In order to investigate the potential mechanism underlying

the effect of apatinib, the study further analyzed the apatinib-treated cells and xenograft tumor tissues. The results revealed a decrease in the expression of p-ERK1/2 and p-AKT consistent with their behavior in thyroid cancer (27), gastric cancer (28), ovarian cancer (29), cholangiocarcinoma (22) and neuroblastoma (30). Previous research also showed that KRAS mutations appeared in 90% of pancreatic cancer patients (31), while RAS-stimulated ERK1/2/MAPK and PI3K/AKT were reported to be active in various pancreatic cancer models (32). In mouse pancreatic cancer cells, the adaptive activation of the classical ERK and PI3K-AKT pathways can also be observed in the early stage after the deletion or inhibition of mTOR kinase (33). Notably, ERK1/2 proteins appear downstream of VEGF activation, regulating cell growth and differentiation and promoting the occurrence and development of pancreatic cancer (34). Moreover, Y1175 is one of the major VEGF-dependent autophosphorylation sites on VEGFR-2 (35). It was reported that inhibition of this domain can lead to the inhibition of phospholipase C-γ in tyrosine phosphorylation as well as significant suppression of MAPK phosphorylation and DNA synthesis (36). Furthermore, the PI3K pathway that is activated by the pY1175 domain is also restricted (37) and downstream AKT subsequently regulates cell growth and survival by phosphorylating various responders. The present study showed that blocking the autophosphorylation of VEGFR-2 as well as the activation of AKT and ERK1/2 results in tumor inhibition. Other studies similarly reported that inhibition of the AKT/mTOR pathway promotes apoptosis and autophagy of pancreatic cancer cells (19), although the present study did not comprehensively analyze this effect. The efficacy of apatinib in patients with advanced pancreatic cancer has also been reported (38,39). In addition, dysregulation of eukaryotic translation initiation factors (eIFs) eIF1, eIF2D, eIF3C and eIF6 and their interaction with the PI3K/AKT/mTOR signaling pathway may serve as prognostic biomarkers for the overall survival of pancreatic cancer patients (40).

In conclusion, the present study showed that apatinib inhibited the viability, proliferation, migration and invasion of pancreatic cells, reducing angiogenesis and growth of the transplanted tumor. These anti-tumor effects possibly occurred due to inhibition of the PI3K/AKT and ERK1/2/MAPK pathways. The results therefore present several novel therapeutic targets for the treatment of pancreatic cancer. Future prospective randomized clinical trials using apatinib as a second-line or higher treatment for pancreatic cancer are therefore needed.

Acknowledgments

Funding: This study was supported by the Clinical Research Award of the First Affiliated Hospital of Xi'an Jiaotong University, China (XJTU1AF-CRF-2015-024) and Institutional Foundation of The First Affiliate Hospital of Xi'an Jiaotong University (2020ZYTS-11).

Footnote

Reporting Checklist: The authors have completed the ARRIVE reporting checklist. Available at https://dx.doi.org/10.21037/tcr-21-207

Data Sharing Statement: Available at https://dx.doi.org/10.21037/tcr-21-207

Conflicts of Interest: All authors have completed the ICMJE uniform disclosure form (available at https://dx.doi.org/10.21037/tcr-21-207). The authors have no conflicts of interest to declare.

Ethical Statement: The authors are accountable for all aspects of the work in ensuring that questions related to the accuracy or integrity of any part of the work are appropriately investigated and resolved. The study was conducted in accordance with the Declaration of Helsinki (as revised in 2013). Experiments were performed under a project license (No. XJTU1AF2015LSL-063) granted by the ethics committee of the First Affiliated Hospital of Xi'an Jiaotong University, in compliance with the national or institutional guidelines for the care and use of animals.

References

1. Bray F, Ferlay J, Soerjomataram I, et al. Global cancer statistics 2018: GLOBOCAN estimates of incidence and mortality worldwide for 36 cancers in 185 countries. CA

Cancer J Clin 2018;68:394-424. Erratum in: CA Cancer J Clin 2020;70:313.
2. Siegel RL, Miller KD, Jemal A. Cancer statistics, 2019. CA Cancer J Clin 2019;69:7-34.
3. Ilic M, Ilic I. Epidemiology of pancreatic cancer. World J Gastroenterol 2016;22:9694-705.
4. Papavasiliou P, Hoffman JP, Cohen SJ, et al. Impact of preoperative therapy on patterns of recurrence in pancreatic cancer. HPB (Oxford) 2014;16:34-9.
5. Mizrahi JD, Surana R, Valle JW, et al. Pancreatic cancer. Lancet 2020;395:2008-20.
6. Mangge H, Niedrist T, Renner W, et al. New diagnostic and therapeutic aspects of pancreatic ductal adenocarcinoma. Curr Med Chem 2017;24:3012-24.
7. Carmeliet P, Jain RK. Molecular mechanisms and clinical applications of angiogenesis. Nature 2011;473:298-307.
8. Carmeliet P, Jain RK. Principles and mechanisms of vessel normalization for cancer and other angiogenic diseases. Nat Rev Drug Discov 2011;10:417-27.
9. Viallard C, Larrivée B. Tumor angiogenesis and vascular normalization: alternative therapeutic targets. Angiogenesis 2017;20:409-26.
10. Li S, Xu HX, Wu CT, et al. Angiogenesis in pancreatic cancer: current research status and clinical implications. Angiogenesis 2019;22:15-36.
11. Zhang Z, Ji S, Zhang B, et al. Role of angiogenesis in pancreatic cancer biology and therapy. Biomed Pharmacother 2018;108:1135-40.
12. Zhao D, Hou H, Zhang X. Progress in the treatment of solid tumors with apatinib: a systematic review. Onco Targets Ther 2018;11:4137-47.
13. Jain RK. Antiangiogenesis strategies revisited: from starving tumors to alleviating hypoxia. Cancer Cell 2014;26:605-22.
14. Ding L, Li QJ, You KY, et al. The use of apatinib in treating nonsmall-cell lung cancer: case report and review of literature. Medicine (Baltimore) 2016;95:e3598.
15. Brower V. Apatinib in treatment of refractory gastric cancer. Lancet Oncol 2016;17:e137.
16. Hu X, Zhang J, Xu B, et al. Multicenter phase II study of apatinib, a novel VEGFR inhibitor in heavily pretreated patients with metastatic triple-negative breast cancer. Int J Cancer 2014;135:1961-9.
17. Scott AJ, Messersmith WA, Jimeno A. Apatinib: a promising oral antiangiogenic agent in the treatment of multiple solid tumors. Drugs Today (Barc) 2015;51:223-9.
18. Tian S, Quan H, Xie C, et al. YN968D1 is a novel and selective inhibitor of vascular endothelial growth factor receptor-2 tyrosine kinase with potent activity in vitro and in vivo. Cancer Sci 2011;102:1374-80.
19. He K, Wu L, Ding Q, et al. Apatinib promotes apoptosis of pancreatic cancer cells through downregulation of hypoxia-inducible factor-1α and increased levels of reactive oxygen species. Oxid Med Cell Longev 2019;2019:5152072.
20. Wu J, Wang J, Su Q, et al. Traditional Chinese medicine Astragalus polysaccharide enhanced antitumor effects of the angiogenesis inhibitor apatinib in pancreatic cancer cells on proliferation, invasiveness, and apoptosis. Onco Targets Ther 2018;11:2685-98.
21. Li J, Wang L. Efficacy and safety of apatinib treatment for advanced esophageal squamous cell carcinoma. Onco Targets Ther 2017;10:3965-9.
22. Huang M, Huang B, Li G, et al. Apatinib affect VEGF-mediated cell proliferation, migration, invasion via blocking VEGFR2/RAF/MEK/ERK and PI3K/AKT pathways in cholangiocarcinoma cell. BMC Gastroenterol 2018;18:169.
23. Lu W, Ke H, Qianshan D, et al. Apatinib has anti-tumor effects and induces autophagy in colon cancer cells. Iran J Basic Med Sci 2017;20:990-5.
24. Liu K, Ren T, Huang Y, et al. Apatinib promotes autophagy and apoptosis through VEGFR2/STAT3/BCL-2 signaling in osteosarcoma. Cell Death Dis 2017;8:e3015.
25. von Marschall Z, Cramer T, Höcker M, et al. De novo expression of vascular endothelial growth factor in human pancreatic cancer: evidence for an autocrine mitogenic loop. Gastroenterology 2000;119:1358-72.
26. Doi Y, Yashiro M, Yamada N, et al. Significance of phospho-vascular endothelial growth factor receptor-2 expression in pancreatic cancer. Cancer Sci 2010;101:1529-35.
27. Meng X, Wang H, Zhao J, et al. Apatinib inhibits cell proliferation and induces autophagy in human papillary thyroid carcinoma via the PI3K/Akt/mTOR signaling pathway. Front Oncol 2020;10:217.
28. Jia X, Wen Z, Sun Q, et al. Apatinib suppresses the proliferation and apoptosis of gastric cancer cells via the PI3K/Akt signaling pathway. J BUON 2019;24:1985-91.
29. Ding J, Cheng XY, Liu S, et al. Apatinib exerts anti-tumour effects on ovarian cancer cells. Gynecol Oncol 2019;153:165-74.
30. Yu X, Fan H, Jiang X, et al. Apatinib induces apoptosis and autophagy via the PI3K/AKT/mTOR and MAPK/ERK signaling pathways in neuroblastoma. Oncol Lett 2020;20:52.

31. Mann KM, Ying H, Juan J, et al. KRAS-related proteins in pancreatic cancer. Pharmacol Ther 2016;168:29-42.
32. Song M, Bode AM, Dong Z, et al. AKT as a therapeutic target for cancer. Cancer Res 2019;79:1019-31.
33. Furukawa T. Impacts of activation of the mitogen-activated protein kinase pathway in pancreatic cancer. Front Oncol 2015;5:23.
34. Hassan Z, Schneeweis C, Wirth M, et al. MTOR inhibitor-based combination therapies for pancreatic cancer. Br J Cancer 2018;118:366-77.
35. Takahashi T, Yamaguchi S, Chida K, et al. A single autophosphorylation site on KDR/Flk-1 is essential for VEGF-A-dependent activation of PLC-gamma and DNA synthesis in vascular endothelial cells. EMBO J 2001;20:2768-78.
36. Estrada CC, Maldonado A, Mallipattu SK. Therapeutic inhibition of VEGF signaling and associated nephrotoxicities. J Am Soc Nephrol 2019;30:187-200.
37. Claesson-Welsh L, Welsh M. VEGFA and tumour angiogenesis. J Intern Med 2013;273:114-27.
38. Liang L, Wang L, Zhu P, et al. Apatinib concurrent gemcitabine for controlling malignant ascites in advanced pancreatic cancer patient: a case report. Medicine (Baltimore) 2017;96:e8725.
39. Li CM, Liu ZC, Bao YT, et al. Extraordinary response of metastatic pancreatic cancer to apatinib after failed chemotherapy: a case report and literature review. World J Gastroenterol 2017;23:7478-88.
40. Golob-Schwarzl N, Puchas P, Gogg-Kamerer M, et al. New pancreatic cancer biomarkers eIF1, eIF2D, eIF3C and eIF6 play a major role in translational control in ductal adenocarcinoma. Anticancer Res 2020;40:3109-18.

Cite this article as: Hu Y, Jing J, Shi Y, Zhang P, Dong D, Wu Y, Dong X, Li E, Fan Y. Apatinib inhibits pancreatic cancer growth, migration and invasion through the PI3K/AKT and ERK1/2/MAPK pathways. Transl Cancer Res 2021;10(7):3306-3316. doi: 10.21037/tcr-21-207

